Ascorbic Acid Modulation of Calcium Channels in Pancreatic β Cells

RAMIN V. PARSEY AND DONALD R. MATTESON

From the Department of Biophysics, University of Maryland School of Medicine, Baltimore, Maryland 21201

ABSTRACT We have studied the effect of ascorbic acid on voltage-dependent calcium channels in pancreatic β cells. Using the whole-cell and perforated-patch variants of the patch clamp technique to record calcium tail currents, we have shown that the slowly deactivating (SD) calcium channel, which is similar to the T-type channel in other cells, is inhibited in a voltage-dependent manner by ascorbic acid (AA). The other channels that carry inward current in β cells, FD calcium channels and sodium channels, are unaffected by AA. Ascorbic acid causes a voltage-dependent decrease in the magnitude of the SD channel conductance which can be explained by the hypothesis that ~50–60% of the channels have their voltage dependence shifted by ~62 mV in the depolarizing direction. Thus, ascorbate appears to modify only a fraction of the SD channels. The activation kinetics of the ascorbate-modified channels are slower than control channels in a manner that is consistent with this hypothesis. Deactivation and inactivation kinetics are unaffected by ascorbate. These effects of ascorbate require metal ions, and it appears that some of the activity of ascorbate is due to a product of its metal catalyzed oxidation, perhaps dehydroascorbate.

INTRODUCTION

Voltage-dependent Ca channels play a crucial role in pancreatic β cell function. Ribalet and Beigelman (1980) provided the first evidence that Ca channels were involved in generating the spikes that dominate the plateau phase of glucose-induced electrical activity. The use of the patch clamp technique to directly measure Ca currents in pancreatic β cells was first reported by Satin and Cook (1985). Since their work, many groups have contributed to our understanding of the properties of Ca channels in β cells from various species, including the adult rat (Hiriart and Matteson, 1988; Sala and Matteson, 1990), neonatal rat (Satin and Cook, 1985), mouse (Rorsman and Trube, 1986; Plant, 1988), guinea pig (Rorsman and Hellman, 1988), and human (Kelly, Sutton, and Ashcroft, 1991). One aspect of the functional importance of Ca channels in β cells involves the suggestion that regulation of Ca channel activity by insulin secretagogues might play a role in modulating insulin secretion (Ashcroft and Rorsman, 1989).

Address correspondence to Dr. Donald R. Matteson, Department of Biophysics, University of Maryland School of Medicine, 660 West Redwood St., Baltimore, Maryland 21201.

J. GEN. PHYSIOL. © The Rockefeller University Press · 0022-1295/93/09/0503/21 $2.00
Volume 102 September 1993 503–523

The existence of multiple types of Ca channels in β cells has been controversial, in part because the result may be species dependent. Initially, tail current analysis was used to describe two populations of Ca channels in rat pancreatic β cells: slowly deactivating (SD) and fast deactivating (FD) Ca channels (Hiriart and Matteson, 1988). This conclusion was later confirmed using single channel recording techniques (Sala and Matteson, 1990; Ashcroft, Kelly, and Smith, 1990). The SD Ca channel has properties similar to the T-type channel found in other preparations (Nowycky, Fox, and Tsien, 1985): it has a small single channel conductance and it activates at relatively negative voltages, inactivates rapidly, and is blocked by low concentrations of Ni^{2+} (Hiriart and Matteson, 1988). The FD channel has properties similar to the L-type Ca channel: it has a single channel conductance of ~25 pS, activates at positive voltages, and inactivates very slowly (Hiriart and Matteson, 1988; Sala and Matteson, 1990). The FD channel is required for generating the upstroke of β cell spikes, but a role for the SD channel has not yet been determined. Because of their relatively negative activation voltage, it is possible that SD channels contribute to the initial upstroke of the membrane potential to the plateau level.

Recently, it has become evident that voltage-dependent Ca channel activity can be modulated by a variety of agents that seem to act by shifting the voltage dependence of a fraction of the channels in the depolarizing direction (Marchetti, Carbone, and Lux, 1986; Bean, 1989; Ikeda, 1991; Beech, Bernheim, and Hille, 1992). In most of these studies it was concluded that the Ca channel type that was modulated was the ω-conotoxin-sensitive N-type channel. In the experiments presented in this article, we now describe another example of this type of regulatory mechanism that involves SD (or T-type) Ca channels. Specifically, we have found that ascorbic acid shifts the voltage dependence of up to 60% of the SD Ca channels by ~62 mV in the depolarizing direction. Because of the known alteration of ascorbic acid metabolism that occurs in diabetes (Chatterjee and Banerjee, 1979; Som, Bosu, Mukherjee, Deb, Choudhury, Mukherjee, Chatterjee, and Chatterjee, 1981), we speculate that this SD Ca channel inhibition could contribute to a reduction in insulin secretion in diabetes.

METHODS

β Cell Culture

All experiments were performed on pancreatic β cells isolated from adult male Sprague-Dawley rats. The method of cell isolation was a modification of the procedure of Lacy and Kostianovsky (1967). The pancreas was perfused with up to 10 ml of Hank's balanced salt solution (HBSS) containing 1 mg/ml BSA, excised, and minced. The tissue was stirred at 37°C for ~30 min in HBSS containing 6 mg/ml of collagenase P (Boehringer Mannheim Corp., Indianapolis, IN). The islets were washed five times with HBSS and subsequently separated from the remaining acinar tissue three to five times with a Lang-Levi pipette. The isolated islets were then dispersed into small clumps and single cells by trituration with a Pasteur pipette in a Spinner solution containing 1 mM EGTA and 10 mg/ml BSA. The cells were then washed several times in RPMI 1640 media supplemented with 10 mg/ml BSA, resuspended in final culture media (RPMI plus 10% fetal bovine serum, 1% glutamine, 100 U/ml penicillin, 100 μg/ml streptomycin, and 50 μg/ml gentamicin), and placed on glass coverslips. Cells were maintained at 37°C in 5% CO_2 and used for no more than 1 wk. It has previously been shown that ~89% of the cells

isolated in this manner are insulin-secreting β cells (Hiriart and Matteson, 1988). All culture solutions were made from powdered salts obtained from Sigma Chemical Co. (St. Louis, MO).

Recording Chamber

For electrical recordings, coverslips with attached β cells were placed into a 200–300-μl plexiglas chamber. Solution flowed into the chamber by gravity at 0.5 to 4 ml/min and was removed by suction via capillary tubes. In perforated-patch experiments, the mouth of the suction tube was covered with a sheet of fine gold mesh (Ted Pella, Inc., Redding, CA) to eliminate vibrations caused by suction. All experiments were performed at room temperature (22–24°C).

Electrodes

Electrodes were pulled from soda-lime glass (VWR micro-hematocrit capillary tubes) in two stages on a Kopf vertical puller (David Kopf Instruments, Tujunga, CA). They were then fire polished to give final electrode resistances of 0.5–2 MΩ when filled with internal solution. For perforated-patch experiments, electrodes had resistances of < 1 MΩ and their tips were filled with nystatin or amphotericin B free solutions and then back filled with the appropriate pipette filling solution. In all experiments, positive pressure was applied to the back of the electrode while it passed through the air–water interface.

Electrophysiological Apparatus

Voltage clamp experiments were done with a slightly modified amplifier of the Matteson and Armstrong design (Matteson and Armstrong, 1986). A Compaq 386 computer was used to control the amplifier through an interface designed and built in our lab. The computer was used to acquire, store, and analyze data using software written in C. With this system it is possible to digitize data with a 16-bit A/D converter at sampling rates up to 100 kHz. Currents were filtered at either 6 or 10 kHz (−3 db) by an 8-pole Bessel filter (Frequency Devices Inc., Haverhill, MA) and sampled at 50 kHz. The holding potential in voltage clamp experiments was −80 mV unless otherwise noted. Cell–pipette junction potentials were not measured nor was any attempt made to correct for these errors. Series resistance compensation was used in all experiments, and was adjusted to the maximum amount possible without causing ringing of the amplifier.

Linear Leak and Capacitance Subtraction

A P/x protocol (Armstrong and Bezanilla, 1974) was used to subtract linear leak and capacitive currents from the total current records. The most commonly used paradigm was one with a sub–holding potential (potential from which control pulses were given) of −120 mV. From this sub–holding potential, two pulses of one-half the amplitude of the test pulse were given. Currents generated by these pulses were added together, and the sum was subtracted from the total current during the pulse. When the test pulse was > 180 mV in amplitude (i.e., to +100 mV from a holding potential of −80 mV) three or four control pulses (of one-third or one-fourth amplitude) were applied in order to avoid underestimation of the SD component of the calcium tail current, which begins to activate at −30 mV. On some occasions, hyperpolarizing pulses were given from a sub–holding potential of −80 mV. If the currents were small or noisy, a modified P/x procedure was used in which 8–30 control pulses of one-third or one-half the amplitude of the test pulse were given, and the responses averaged. This procedure produced much lower noise levels than the paradigm in which only two to four control pulses

were given. In some cases the displayed currents are averages of two to three identical pulses applied successively; i.e., they are signal averaged.

Solutions

The external solution contained (mM) 136 NaCl, 10 $CaCl_2$, 10 HEPES, and 200 nM TTX (pH adjusted to 7.4 with NaOH). In some experiments the external solution also contained 500 nM $CuSO_4$. For experiments done in whole-cell mode, the internal solution contained (mM) 30 CsCl, 100 Cs glutamate, 2 $MgCl_2$, 10 EGTA, 10 HEPES, 4 MgATP, and 200 μM NaGTP (pH adjusted to 7.2 with CsOH). In perforated-patch experiments, the internal solution contained (mM) 55 CsCl, 70 $CsSO_4$, 7 $MgCl_2$, and 10 HEPES (pH adjusted to 7.2 with CsOH). When amphotericin B was used to create the perforations, a 60 mg/ml stock solution in DMSO was made fresh each day. From the stock solution 12 μl was added to 3 ml of the internal solution. The solution was triturated with a Pasteur pipette several times and then sonicated for 30–60 s. This solution was used for up to 4 h. If nystatin was used, a 25 mg/ml stock was made in DMSO, stored at −4°C in the dark, and used for as long as 1 wk. From this stock, 12 μl was diluted into 3 ml of the internal just before use. This solution was used for up to 5 h. In some experiments the dispersant pluronic (Molecular Probes, Inc., Eugene, OR) was used to accelerate the incorporation of nystatin into the membranes. A stock was made by heating 25 mg of pluronic in 1 ml of DMSO at 37°C for 10 min. This solution was stored at −4°C in the dark and used for up to 1 mo. The stock was diluted to 0.05% in the pipette filling solution containing nystatin before being used. It was not necessary to sonicate this solution.

RESULTS

Calcium Currents in Pancreatic β Cells

Calcium currents recorded from rat pancreatic β cells in whole-cell patch clamp experiments are illustrated in Fig. 1. The pulse protocol used to generate these currents is displayed at the top of the figure. During the 9-ms pulse the current activates relatively slowly and does not inactivate. Upon returning the membrane potential to −80 mV, the tail current declines rapidly at first and then more slowly. The two phases of the tail current are due to the closure, or deactivation, of two distinct populations of calcium channels that differ not only in their deactivation rates but also in their inactivation rates, activation voltages, selectivity, and sensitivity to rundown (Hiriart and Matteson, 1988). Due to their deactivation rates and similarity to calcium currents seen in GH3 cells (Matteson and Armstrong, 1986), we refer to these currents as slowly deactivating (SD) and fast deactivating (FD) calcium currents.

Analysis of Tail Currents

The method used to analyze the SD and FD tail currents is illustrated in Fig. 1, *B* and *C*. To obtain separate measures of the SD and FD components that contribute to the tail current, the data are fit by the sum of two exponentials (solid line in Fig. 1 *B*) according to the following equation:

$$I = A \exp\left(-\frac{t}{\tau_{FD}}\right) + B \exp\left(-\frac{t}{\tau_{SD}}\right) + C \quad (1)$$

where A, τ_{FD}, B, and τ_{SD} are the initial amplitudes and time constants of the fast and slow components, respectively, and C is a constant. The fitting routine is an iterative

procedure that uses a Levenberg-Marquardt routine to minimize the sum of squared errors between the data and the fit. The initial amplitude of the slow exponential (parameter *B* from the fit) is used as a measure of the magnitude of the instantaneous SD tail current. The maximum of the data remaining after the slow component is subtracted from the total current (Fig. 1 *C*) is used as a measure of the FD component of the tail. The initial amplitude of the fast component from the fit is not used as a measure of the FD component because of the potentially large error in fitting such a fast process which may only be represented by a few points. These

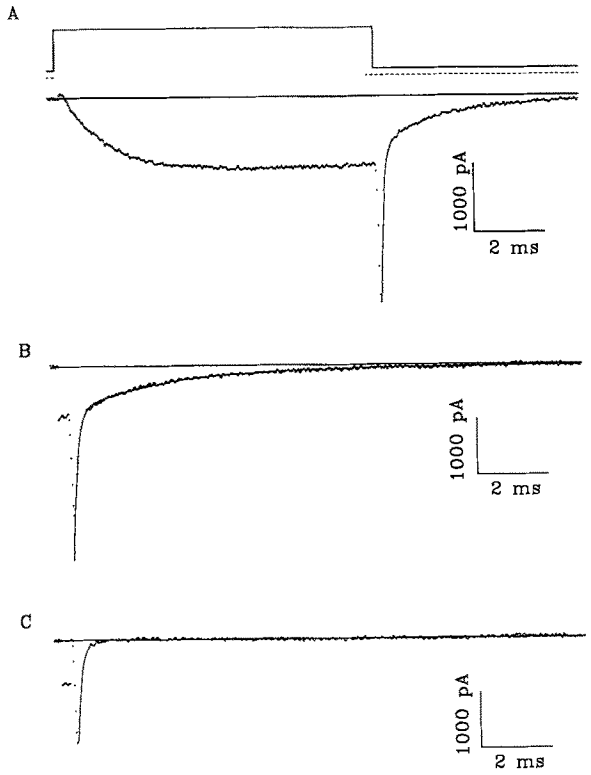

FIGURE 1. Calcium currents in pancreatic β cells. (*A*) Whole-cell current recorded in response to a 9-ms depolarization to +20 mV from a holding potential of −80 mV. Data were sampled throughout the protocol illustrated at the top. (*B*) Tail current recorded after a 10-ms depolarization to +10 mV (*dotted trace*). The dashed line under the pulse protocol indicates when data was sampled for tail current recordings. The first 10 data points are taken before the pulse and sampling is then turned off. Sampling is turned back on just before the end of the pulse, and continues while the membrane potential is returned to −80 mV. The smooth, solid line is a fit of Eq. 1 to the data. (*C*) Same data as in *B*, with the slow exponential component subtracted out.

estimates of the maximum amplitudes of the SD and FD tail currents can be used to generate conductance–voltage relationships, as described below.

Conductance–Voltage Relationships

The conductance–voltage (*G-V*) relationship has been used to characterize the voltage dependence of various types of channels (cf. Hodgkin and Huxley, 1952). Because the amplitude of the tail current is a measure of the conductance activated during the preceding pulse, SD and FD tail current components can be used as estimates of the conductances activated in response to a series of activating pulses. In the experiment illustrated in Fig. 2, tail currents were recorded in response to 10-ms test pulses of variable amplitude (Fig. 2 *A*), and the normalized SD and FD

amplitudes were plotted as a function of test pulse voltage (Fig. 2 *B*). At relatively negative voltages, the tail current is entirely due to SD channels. With progressively larger voltages, the FD current appears and the SD current saturates. At the highest voltages, the FD tail current also saturates.

The SD and FD *G-V*'s in Fig. 2 were fit by a two-state Boltzmann equation in order to estimate the voltage where half of the channels are open, and the slope factor. The slope factor can be used to place a lower limit on the magnitude of the total equivalent gating charge that moved to open the channel (Hille, 1992). These

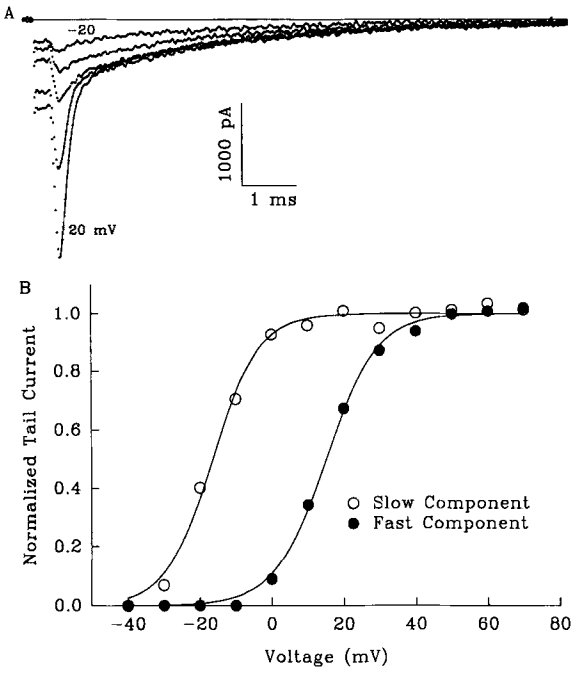

FIGURE 2. SD and FD voltage dependence of activation. (*A*) Whole-cell tail currents recorded after 10-ms depolarizations to −20, −10, 0, 10, and 20 mV. Solution B. (*B*) Tail current amplitudes were normalized and plotted vs. voltage to compare the voltage dependence of SD and FD conductance. The smooth lines are fits of Eq. 2 to the data. Parameters for the SD component were $V_{1/2} = -16.4$, $s = 6.50$, and for the FD component $V_{1/2} = 15.1$, $s = 7.17$.

parameters help to characterize the steady-state voltage dependence of the channel activation process. The two-state Boltzmann equation has the following form:

$$G(V) = \frac{G_{max}}{1 + \exp\left[-\frac{(V - V_{1/2})}{s}\right]} \tag{2}$$

where $G(V)$ is the steady-state conductance at V mV, G_{max} is the maximum conductance, s is the slope factor, and $V_{1/2}$ is the voltage at which half of the channels are in the open state. The slope factor is equal to kT/ze, where k is Boltzmann's constant, T is the temperature, e is the electronic charge, and z is the magnitude of the equivalent gating charge. As illustrated in Fig. 2, the data for both the SD and FD channels are well fit by this equation, and the parameters of the fit are given in the figure legend.

Effect of Ascorbic Acid on SD Calcium Currents

Application of ascorbic acid to pancreatic β cells causes a voltage-dependent change in the amplitude of the SD component of the calcium tail current, as shown in Fig. 3. At −10 mV only SD channels are activated and therefore the tail current has only a slow component (Fig. 3 *A*). This SD tail current is reduced ~50% by 1 mM ascorbate (Fig. 3 *A*). However, at more positive potentials (+50 mV in the case of Fig. 3 *B*) there is no difference between the control and ascorbate tail currents recorded from this same cell. This reduction in the amplitude of the SD tail current becomes apparent within 30 s after adding ascorbate, and reaches steady state in ~3–4 min. Although 1 mM ascorbate was used in this experiment, concentrations as low as 50 μM produced a measurable effect.

To more fully characterize the voltage-dependent change in SD current amplitude, *G-V* relationships were generated with and without ascorbate, as illustrated in Fig.

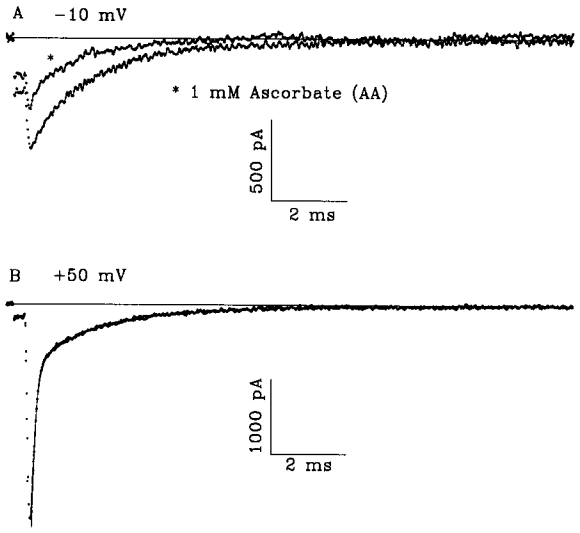

FIGURE 3. Ascorbate modulation of SD calcium tail currents. (*A*) The SD tail current recorded in response to a 10-ms depolarization to −10 mV. In the presence of 1 mM ascorbate, there is a 50% reduction in the current amplitude. (*B*) In the same cell, the tail current after a depolarization to +50 mV is identical in control and ascorbate. Whole-cell experiment.

4 *A*. In this experiment, 50 μM ascorbate reduced the SD tail currents by ~50% at −10, 0, or +10 mV. As the cell is further depolarized, the magnitude of the current reduction becomes smaller. In the cell shown in Fig. 4, there is only a 16% reduction in the amplitude of the current at +70 mV. This effect of ascorbate on the SD *G-V* relationship was observed using various ascorbate concentrations and a number of different patch clamp configurations. The effect was found in five whole-cell experiments using 50 μM ascorbic acid, six whole-cell experiments using 100 μM ascorbic acid, and in 58 experiments using 1 mM ascorbate in the following patch-clamp configurations: whole-cell (n = 20), nystatin perforated patch (n = 13), and amphotericin perforated patch (n = 25).

Most ascorbate experiments were conducted with the perforated-patch technique for several reasons. First, stable recordings of Ca currents for periods of up to 1 h were more consistently obtained using the perforated-patch technique. Second, in

most whole-cell experiments, exposure of the cell to ascorbate caused an irreversible increase in the holding current, which interfered with the accurate recording of calcium currents. This effect was much less frequent when the experiments were done using the perforated-patch technique.

Ascorbate Has No Effect on FD Calcium Currents or Sodium Currents

We were interested in determining if the effect of ascorbate is specific for SD Ca channels. To test for an effect on FD Ca channels we constructed *G-V* curves for the fast component of the Ca tail currents. Fig. 4 *B* illustrates a *G-V* curve for the FD current from the same cell as in Fig. 4 *A*, and it shows that there is little or no effect of ascorbate on the FD calcium current at any of the measured voltages. Similar

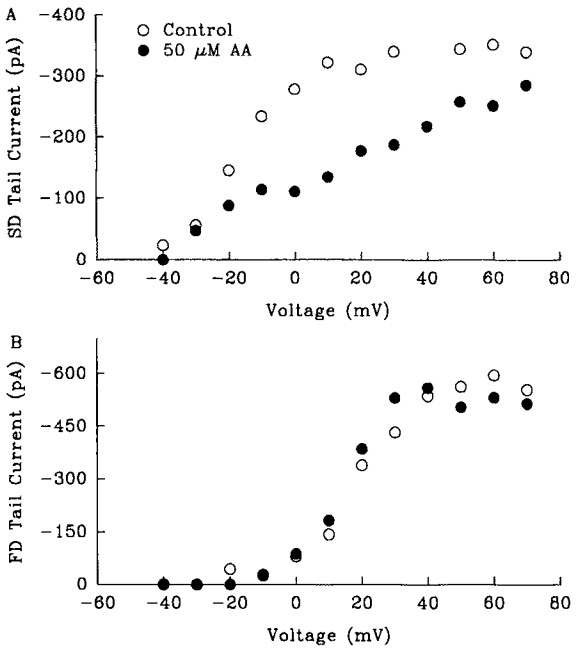

FIGURE 4. FD and SD *G-V* relationships in ascorbate. (*A*) The effect of 50 μM ascorbate on the SD *G-V* is illustrated. There is a large reduction in tail current amplitudes after depolarizations to −10 mV (51%) and 0 mV (60%). The current approaches control levels as the cell is depolarized further (i.e., there is a 16% reduction at +70). (*B*) The FD *G-V* in the same cell as in *A*. Ascorbate does not affect the FD calcium current. Whole-cell experiment.

results have been obtained in other cells at concentrations of ascorbate up to 1 mM. On some occasions, a small (5–10%) increase in the FD current amplitude has been observed at all voltages. When experiments were conducted in the absence of TTX, there was little or no change in the sodium current produced by ascorbate (data not shown). Thus, at concentrations up to 1 mM, ascorbate produces a significant and reproducible modulation of only the SD calcium channel, and not FD calcium or sodium channels.

The Ascorbate Effect Requires Heavy Metal

There are several reactions in which the presence of metal is either required for, or enhances, the effect of ascorbate (Samuni, Aronovitch, Godinger, Chevion, and

Czapski, 1983; Stadtman, 1991). Therefore, a series of experiments was performed to test for the requirement of heavy metals in the effect of ascorbate on the SD calcium current. Our goal in these experiments was to remove metal ions with a chelator and then test for an ascorbate effect in the absence of metal ions. Before doing this experiment, we first examined the direct effects produced by metal ions and/or the chelator. To standardize the heavy metal concentration in our solutions we made a stock of deionized water to be used in this entire series of experiments, and added 500 nM copper to all external solutions. The effect of this concentration of copper on SD channels is illustrated in Fig. 5 *A*, which shows the *G-V* relationships before and

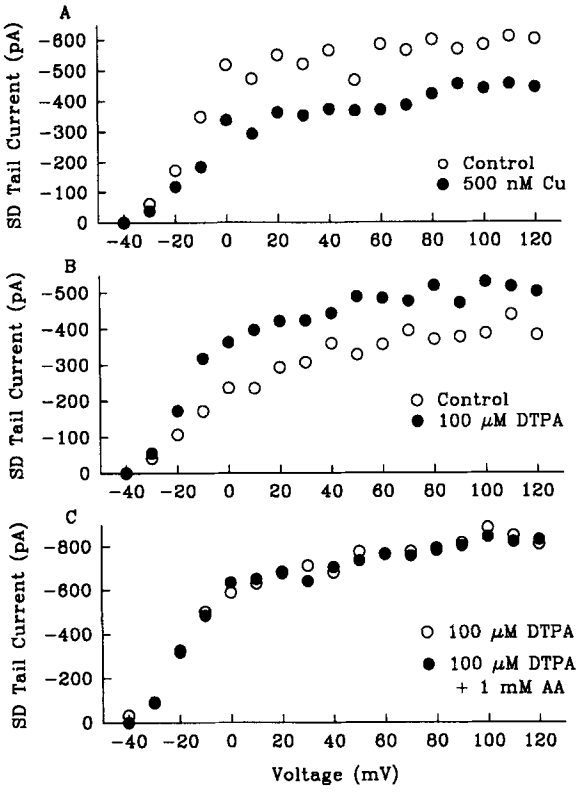

FIGURE 5. The ascorbate effect is blocked by DTPA. In all panels the SD tail current amplitude is plotted as a function of the activating voltage. (*A*) 500 nM copper decreases the SD current amplitude at all voltages. This result was seen in three other cells with an average decrease of 20.0 ± 5.29%. In the experiments shown in *B* and *C*, 500 nM copper sulfate was present in all external solutions. (*B*) A different cell exposed to 100 μM DTPA. There is an increase in amplitude of the tail currents at every voltage. Similar results were seen in five other cells with a average increase of 30.7 ± 10.1%. (*C*) This cell was exposed to 100 μM DTPA and then to 100 μM DTPA plus 1 mM ascorbate. The ascorbate-induced voltage-dependent modulation of the SD current is not seen (cf. Fig. 4 *A*). Similar results were seen in three other cells. Whole-cell experiments.

after the addition of 500 nM copper. The SD tail current amplitude is decreased at all voltages. The average decrease in the maximum SD current amplitude was 20.0 ± 5.29% (n = 4). Various metal ions are known to block calcium currents (Hiriart and Matteson, 1988; Akaike, Kostyuk, and Osipchuk, 1989; Chow, 1991; Winegar, Kelly, and Lansman, 1991), so this result probably reflects SD channel block by copper. Therefore, removal of heavy metals should increase the current. Diethylenetriamine-penta-acetic acid (DTPA) binds heavy metals with high affinity (i.e., K_D of 10^{-21} for copper) without significantly binding calcium (Martell and Smith, 1977). The

addition of 100 μM DTPA increased the SD conductance at all voltages (Fig. 5 *B*). In six cells, 100 μM DTPA increased the maximum current amplitude 30.7 ± 10.1%.

Finally, to test for the requirement of heavy metals in the ascorbate effect, we used ascorbate in conjunction with DTPA. When the free metal is chelated by DTPA, ascorbate in the presence of DTPA does not produce the voltage-dependent modulation of the SD channel (Fig. 5 *C*). Similar results were obtained in three other cells. These experiments strongly suggest that the effect of ascorbic acid on the voltage-dependent inhibition of SD channels requires metal. Therefore, most of the remaining experiments in this paper have been performed in the presence of 500 nM copper.

A typical experiment using 500 nM copper and 500 μM ascorbate is shown in Fig. 6. In this experiment, 500 μM ascorbate was applied first, and produced two effects:

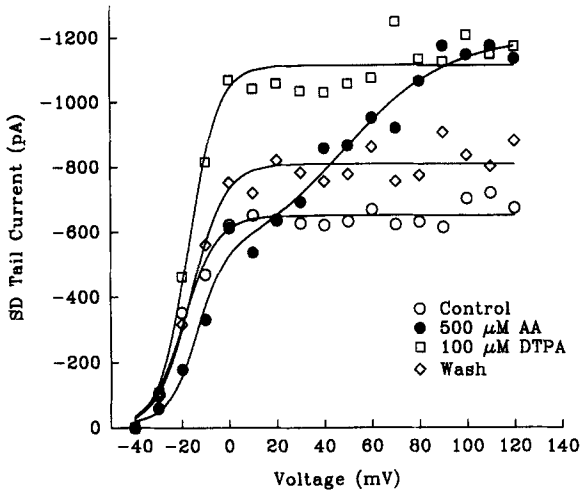

FIGURE 6. The ascorbic acid effect in the presence of added copper. In this experiment all solutions contained 500 nM copper sulfate. After the control *G-V* (*open circles*) was generated the cell was exposed to 500 μM ascorbate. When the ascorbate effect had reached steady state, a second *G-V* was taken (*filled circles*). The external solution was then switched back to control. In this cell not enough time was allowed for the effect to completely wash out, but it can be seen that the shift in the voltage dependence is clearly reversed (*open diamonds*). At this point the cell was exposed to 100 μM DTPA (*open squares*) and there was an increase in the current at all voltages. Similar results were seen in three other cells. Amphotericin perforated-patch experiment.

(*a*) a voltage-dependent inhibition of the SD current similar to that shown in Fig. 4 (evidenced here by the fact that the current doesn't saturate until +90 mV) and (*b*) an increase in the maximum amplitude of the SD current. These results indicate that, in the presence of added copper, ascorbate has at least two clear effects on SD calcium channels: a shift in the voltage dependence of a fraction of the channels similar to that shown in Fig. 4 *A*, and an increase in the maximum magnitude of the SD current. Both effects are reversible (n = 10), although in this particular experiment sufficient time was not allowed for the ascorbate effect to reverse completely.

The increase in the magnitude of the SD current could be due to a relief of copper block of the channels via chelation of the metal by ascorbate or one of its breakdown products (e.g., oxalate). The DTPA curve in Fig. 6 supports this hypothesis. After the cell was exposed to ascorbate, 100 μM DTPA was applied and a third *G-V* was measured. DTPA caused an increase in the total magnitude of the current at every

voltage, but did not produce a change in voltage dependence like that seen in ascorbate. The maximum amplitude of the DTPA curve is nearly identical to that in ascorbate, suggesting that if these agents are indeed acting via metal chelation, then both chelators, DTPA and ascorbate (or the ascorbate breakdown product), are chelating all available metal.

Two Components in the G-V Relationships in Ascorbate

In the presence of ascorbate, the SD conductance appears to increase in two stages as the voltage increases. At negative voltages, −40–0 mV, the SD conductance increases rapidly but then tends to plateau near 0 mV. Further increases in voltage again increase the conductance until it saturates at about +100 mV (Fig. 7 *A*). This biphasic

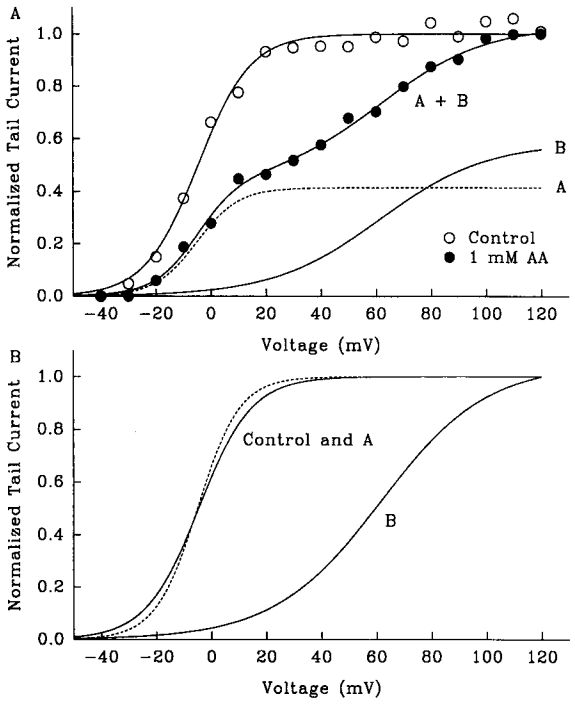

FIGURE 7. Fitting the ascorbate data with the sum of two Boltzmann distributions. (*A*) The control SD *G-V* (*open circles*) is fit with a single, two-state Boltzmann equation (Eq. 2). The ascorbate data (*filled circles*) is fit by the sum of two Boltzmann distributions using Eq. 3 in the text (solid line labeled *A* + *B*). To better illustrate the contributions of each Boltzmann, they are plotted separately as *A* and *B*. (*B*) The control Boltzmann (*solid line*) and curve *A* from the ascorbate data (*dashed line*) are scaled for comparison. Amphotericin perforated-patch experiment.

G-V relationship suggested to us the existence of two populations of SD channels in the presence of ascorbate. The component between −40 and about +20 mV is similar in voltage dependence to control SD channels, whereas the second component starts at about +20 mV and saturates at about +100 mV. Under the assumption of two populations of channels with different voltage dependencies, the ascorbate *G-V* should be described by the sum of two Boltzmann distributions according to the following equation:

$$G(V) = \frac{G_1}{1 + \exp\left(-\frac{V - V_1}{s_1}\right)} + \frac{G_2}{1 + \exp\left(-\frac{V - V_2}{s_2}\right)} \quad (3)$$

where G_1 and G_2 are the maximum conductances and V_1, V_2, s_1, and s_2 are the $V_{1/2}$ and slope factors for the two Boltzmann distributions. The solid line labeled $A + B$ in Fig. 7 A is the fit of this equation to the SD G-V recorded in the presence of ascorbate.

To further illustrate the fit, the contribution of each Boltzmann distribution is shown separately as the curves labeled A and B in Fig. 7 A. In this particular cell, the parameters that best described the control data were a $V_{1/2}$ of -4.65 mV and a slope factor of 9.67. These values were very similar to values obtained for the A curve in ascorbate: -5.08 for the $V_{1/2}$ and 7.68 for the slope factor. In fact, curve A appears to be a scaled version of the curve that is fit to the control data (Fig. 7 B), so these channels appear to be unmodified by ascorbate. The second Boltzmann curve appears to be due to a fraction of channels that have been modified by ascorbate (curve B in Fig. 7 A). The $V_{1/2}$ for the modified channels is 56.8 mV, which is 61.4 mV more depolarized than for the control channels. Furthermore, the G-V curve for the ascorbate-modified channels was less steep than for normal channels; the slope factor was 19.5 in ascorbate versus 9.67 in control, indicating that there is a decrease in the total gating charge associated with the closed to open transition of the channel. Table I gives the parameters obtained from fitting Eq. 3 to the data from six cells recorded under identical conditions (amphotericin perforated-patch experiments with 500 μM ascorbate and 500 nM copper). The average change in $V_{1/2}$ between control and ascorbate-modified channels was 62.4 mV.

To summarize, we believe that there are two populations of SD channels in the presence of ascorbate. One population of channels in ascorbate is nearly identical in voltage dependence to control channels, while the second population has its voltage dependence shifted by ~62 mV in the depolarizing direction. Such a shift in voltage dependence would probably be accompanied by a change in the gating kinetics of the channels. Therefore, we studied SD channel gating behavior in terms of activation, deactivation, and inactivation kinetics.

Activation Kinetics

To test the hypothesis that the ascorbate-modified channels had altered activation kinetics, we performed the following experiments. The voltage protocol displayed at the top of Fig. 8 was used to measure SD channel activation kinetics. Tail currents were measured after depolarizing pulses of variable duration (Fig. 8 A). The amplitude of the SD tail current increases as the duration of the pulse is increased, reflecting the activation of a larger number of SD channels. With longer depolarizations, the SD current starts to decrease, or inactivate, a well-characterized property of SD channels in β cells (Hiriart and Matteson, 1988). A plot of the tail current amplitude versus the activating pulse duration (Fig. 8 B) reflects the activation and inactivation gating of the SD channels. The smooth curve superimposed on the data is the fit of a model which is described in the Discussion.

In terms of the hypothesis of two SD channel populations in ascorbate, we would predict that with small depolarizations only normal channels would be activated, so that the activation kinetics should be identical to control. Fig. 9 A shows that when the activation kinetics are measured in response to a depolarizing pulse to -10 mV (where few ascorbate-modified channels should be activated), the rate of activation is not significantly affected by ascorbate. However, when activation is measured at +90

mV, ascorbate appears to decrease the rate of SD channel opening (Fig. 9 *B*). At positive voltages in the presence of ascorbate, both modified and unmodified channels are activated, and the results suggest that not only do the modified channels have their voltage dependence shifted by ~62 mV, but they also activate more slowly than normal channels. Slowing of activation kinetics at +90 mV in the presence of ascorbate was observed in 13 cells. This effect is quantified using the kinetic modeling presented in the Discussion.

TABLE I

Parameters of G-V Fits in Control and Ascorbate

Cell	Control*		Ascorbate‡		
	$V_{1/2}$	Slope factor	Percent§	$V_{1/2}$	Slope factor
1	−10.3	18.5	29.6	−19.5	6.89
			70.4	38.5	23.2
2	−12.0	9.21	44.0	−12.8	10.6
			56.0	46.1	15.7
3	−7.32	15.7	51.4	−4.28	10.7
			48.6	63.0	17.6
4	−19.3	7.13	41.0	−13.8	5.8
			59.0	47.7	22.4
5	−9.62	12.4	41.2	−12.5	9.17
			58.8	55.0	23.7
6	−6.03	16.2	41.2	−2.97	12.8
			58.8	59.3	19.3
Averages ± SD	−10.8 ± 4.70	13.0 ± 4.61	41.4 ± 7.00	−11.0 ± 6.26	9.32 ± 2.62
			58.6 ± 7.00	51.6 ± 9.13	20.3 ± 3.27

*Parameters listed are for the control *G-V* relationship.

‡The first row lists the parameters for the channel population present at low voltages (unmodified channels), and the second row lists those for the "modified channels."

§Percent refers to the percentage of the total SD conductance due to this component and is calculated as G_1 or G_2 divided by $G_1 + G_2$ (cf. Eq. 3).

Deactivation Kinetics

To characterize SD channel deactivation kinetics, the time constant of the SD tail current was measured after pulses to different voltages. The strategy in this experiment was similar to that of the activation kinetics: in ascorbate, channels that are opened at −10 mV should be similar to control channels, whereas the channels opened at +90 mV should be roughly half normal channels and half modified channels. Average SD tail current time constants in control and ascorbate in response

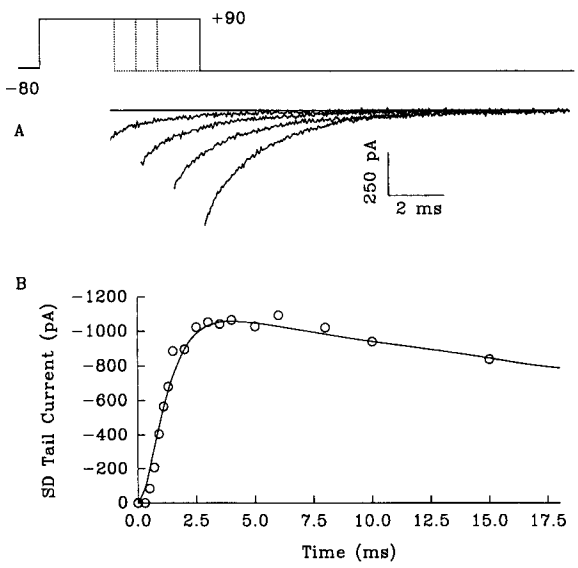

FIGURE 8. SD current activation kinetics. The pulse protocol used to characterize SD channel activation is shown at the top of the figure. Depolarizing pulses of varying duration are given and the tail current is recorded upon repolarization. (*A*) SD tail currents recorded in response to 0.7-, 0.9-, 1.1-, and 1.5-ms duration pulses to +90 mV. The first 1.4–1.5 ms of the tail currents (FD tail current) is not shown. (*B*) The symbols plot the SD tail current amplitude versus pulse duration. The smooth curve is the fit produced by a model presented in the Discussion. Amphotericin perforated-patch experiment.

to three different activation voltages are presented in Table II. The cells are the same six cells that were presented in Table I. The time constants in control and ascorbate are comparable in all cases. Thus, although ascorbate slows activation kinetics, it has no effect on deactivation kinetics.

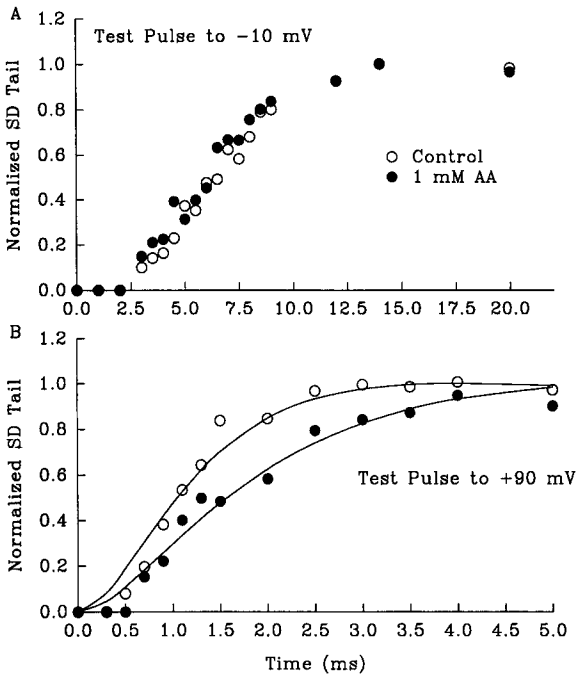

FIGURE 9. Ascorbate slows activation at +90 mV without affecting activation at −10 mV. Activation kinetics were measured as shown in Fig. 8. Open circles are the control data and filled circles are in the presence of 1 mM ascorbate. When the depolarizing test pulse is to −10 mV (*A*), there is no difference in control versus ascorbate. However, when the pulse is to +90 mV (*B*), there is a slowing of the activation rate in ascorbate. The significance of the curves is discussed in the text. Amphotericin perforated-patch experiment.

TABLE II

Deactivation Time Constants in Ascorbate (n = 6)

Test pulse amplitude	Control τ_{dea} ± SD	Ascorbate τ_{dea} ± SD
mV	*μs*	*μs*
−10	2,476 ± 821	2,215 ± 627
+40	2,515 ± 730	2,634 ± 791
+90	2,720 ± 710	2,688 ± 1,060

Inactivation Kinetics

We have also examined the effect of ascorbate on SD channel inactivation using the pulse protocol illustrated at the top of Fig. 10. A variable duration prepulse is given to inactivate some of the channels. A 7-ms test pulse is then given to +90 mV and the amplitude of the subsequent tail current is used as a measure of the noninactivated channels. Currents recorded in response to this protocol are illustrated in Fig. 10*A*. As the duration of the depolarizing prepulse is increased, the amplitude of the slow component decreases because some channels become inactivated during the prepulse. Prepulses of varying duration were given to −10 mV, where theoretically all the channels are identical to the control channels, and to +90 mV, where there is a mix of control and ascorbate-modified channels. The amplitudes of the tail currents are normalized in Fig. 10 in order to compare the rates of inactivation. The results show that there is no difference between control and ascorbate in the rate of channel

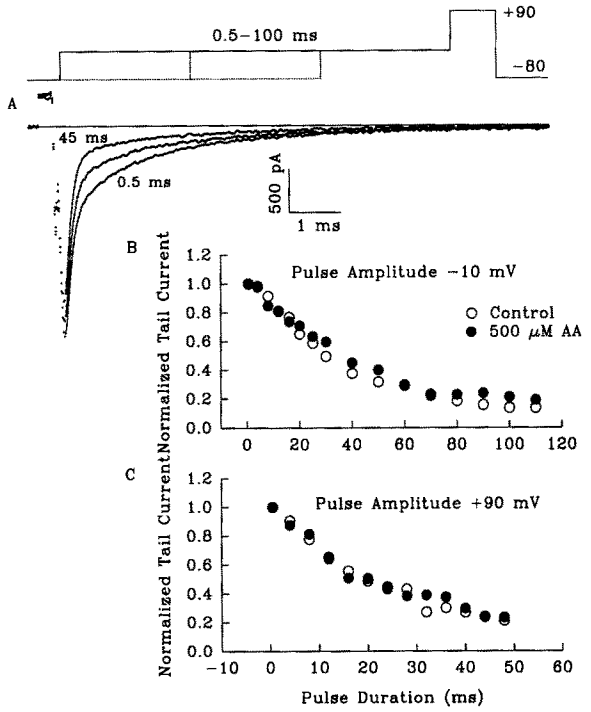

FIGURE 10. Ascorbate does not affect inactivation kinetics at −10 or +90 mV. The pulse protocol used is displayed at the top of the figure. Prepulses were given to either −10 or +90 mV for varying durations, followed by a 7-ms test pulse. (*A*) Tail currents recorded after prepulses of 0.5, 15, and 45 ms to −10 mV. SD tail current amplitude is plotted as a function of prepulse duration for pulses of −10 mV (*B*) and +90 mV (*C*). Open circles are control and filled circles are in 500 μM ascorbate. Data are normalized to compare rates of inactivation. Amphotericin perforated-patch experiment.

inactivation in response to prepulse depolarizations to −10 mV (Fig. 10 *B*) or to +90 mV (Fig. 10 *C*). These data are well fit by a single exponential, and the time constant of this exponential (τ_{ina}) provides an estimate of the rate of inactivation. Table III shows the average τ_{ina} at these two voltages in control and ascorbate. Clearly, there is no significant effect of ascorbate on SD channel inactivation kinetics.

In summary, our data suggest that ascorbic acid modifies 50–60% of the pancreatic β cell SD-type Ca channels by shifting their activation voltage dependence by ~62 mV compared with the native channels. The rate of activation of ascorbate-modified channels is slower than normal, but deactivation and inactivation kinetics are not altered at any of the measured voltages.

TABLE III

Inactivation Time Constants in Control and Ascorbate (n = 4)

Test pulse amplitude	Control τ_{ina} ± SD	Ascorbate τ_{ina} ± SD
	ms	*ms*
−10 mV	31.9 ± 7.70	36.7 ± 7.07
+90 mV	21.3 ± 4.20	24.7 ± 6.91

τ_{ina} measured over the range of 0.5–110 ms at −10 mV and 0.5–48 ms at +90. Three cells in 500 μM ascorbate + 500 nM copper, one in 1 mM ascorbate. All cells displayed the voltage-dependent effect of ascorbate.

DISCUSSION

Voltage-dependent Modulation of Ca Channel Activity

Recent evidence suggests that modulation of calcium channel activity by a shift in the voltage dependence of activation may be a general type of Ca channel regulation. Several groups have reported biphasic *G-V* relationships in response to a variety of neurotransmitters (Bean, 1989; Beech et al., 1992). Bean (1989) has suggested that the biphasic *G-V* relationship, which he found in the presence of norepinephrine, is produced by two modes of Ca channel gating, which he refers to as a "willing" mode and a "reluctant" mode. Channels in the willing mode open in response to small depolarizations, while the channels in the reluctant mode require large depolarizations to open. Quantitatively, the $V_{1/2}$ for the willing channels was about −15 mV, whereas that for the reluctant channels was about 62 mV, and the reluctant channels had a somewhat less steep voltage dependence. Neurotransmitters are thought to act by shifting channels from the willing mode to the reluctant mode. A second important effect of neurotransmitters is that they produce a slow activation phase of the Ca current (Marchetti et al., 1986; Bean, 1989; Elmslie, Zhou, and Jones, 1990), which is thought to be due in part to conversion of reluctant channels to willing channels (Bean, 1989; Elmslie et al., 1990).

In many respects the effects of ascorbate on Ca currents in pancreatic β cells are similar to the effects of neurotransmitters in neurons, but there are several important differences. First of all, in our experiments the channel being modulated is the low voltage–activated, fast inactivating SD (or T) type Ca channel. In neurons, others

have concluded that a high voltage–activated N-type channel is specifically modulated by neurotransmitters (Hirning, Fox, McClesky, Olivera, Thayer, Miller, and Tsien, 1988; Bean, 1989). Thus, it may turn out that voltage-dependent regulation of Ca channel activity may involve different populations of Ca channels in different cell types. Secondly, we never observed a slow activation phase of the SD current in the presence of ascorbate. It is possible that a slow activation phase might be obscured by the relatively fast inactivation of these channels. If this were the case, inactivation in the presence of ascorbate would appear slower than control, but in fact it was unchanged (Fig. 10). Thus, our experiments provided no evidence for fast interconversion between normal channels and ascorbate-modified channels. Finally, neurotransmitter-induced inhibition of Ca channels in neurons involves G proteins (Tsien, Lipscombe, Madison, Bley, and Fox, 1988). Although we have not explored this point exhaustively, we have found that ascorbate inhibits the SD channels in cells that have been well dialyzed without GTP in the patch pipette, suggesting that G proteins are not involved.

A Kinetic Model of the Ascorbate Effect

Many of the biophysical effects produced by ascorbate are similar to the reported effects of diethylpyrocarbonate (DEP) on K channels in squid giant axons. For example, DEP shifted the K channel steady-state activation curve to more positive voltages, slowed K channel opening, and had little or no effect on channel closing (Spires and Begenisich, 1990). Furthermore, these authors could account for the DEP effects with a simple kinetic model in which DEP selectively affects a slow, weakly voltage-dependent activation step. In this section, we present a simple kinetic model of the SD Ca channel, in which the effect of ascorbate can be accounted for by a change in a voltage-dependent transition between two closed states of the channel.

The simplest kinetic model that will describe SD channel gating is one with two closed states (to explain the delay in channel activation), a single open state, and a single inactivated state. We therefore used the following state diagram to describe the gating behavior of the SD channel:

$$C_2 \underset{\beta_1}{\overset{\alpha_1}{\rightleftharpoons}} C_1 \underset{\beta_2}{\overset{\alpha_2}{\rightleftharpoons}} O \underset{\beta_3}{\overset{\alpha_3}{\rightleftharpoons}} I$$

where C_2 and C_1 represent the two closed states, O represents the open state, I represents the inactivated state, and the α's and β's are first-order rate constants governing transitions between the states. The following paragraphs describe our use of this model to fit SD channel gating kinetics and to account for the effects of ascorbate on channel gating.

FITTING THE CONTROL DATA

To fit the SD channel activation time course, we derived an expression for the fraction of channels open as a function of time. The general solution for this reaction scheme with four states has the form:

$$O(t) = A + B \exp(-t/\tau_1) + C \exp(-t/\tau_2) + D \exp(-t/\tau_3) \quad (4)$$

where the time constants (τ_1, τ_2, and τ_3) and the constants A, B, C, and D are

functions of the six rate constants in the model. To fit this equation to SD channel gating kinetics, we used the following procedures to estimate the six rate constants.

Estimation of α_3 and β_3. SD channel inactivation kinetics are very slow compared with activation (cf. Fig. 8). We have therefore made the simplifying assumption that the inactivation data shown in Fig. 10 reflect a first-order process that can be described with the following relationships for τ_{ina} and I_∞ (the fraction of channels inactivated in the steady state): $\tau_{ina} = 1/(\alpha_3 + \beta_3)$ and $I_\infty = \alpha_3/(\alpha_3 + \beta_3)$. Previous results have demonstrated that SD channel inactivation is independent of voltage (Fig. 10). The average values of τ_{ina} and I_∞ in our experiments were 28.6 ms and 0.78, which give values of 0.027 ms^{-1} for α_3 and 0.008 for β_3. These values were used in subsequent calculations involving the model.

Calculation of β_1 and β_2 from α_1 and α_2. It can be shown that for a voltage-dependent transition, the ratio of the forward to backward rate constant can be described by the following relationship:

$$\frac{\alpha}{\beta} = \exp\left(\frac{V - V_{1/2}}{\frac{kT}{ze}}\right) \tag{5}$$

where k is the Boltzmann constant, T is the temperature in Kelvin, z is the valence of the gating charge that moves in the transition between the two states, e is the electronic charge, and $V_{1/2}$ is the voltage at which $\alpha = \beta$. Given a value for α_1 or α_2, this equation could be used to calculate β_1 or β_2. To use Eq. 5, values for z and $V_{1/2}$ for each activation step are needed.

(*a*) Estimating z_1 and z_2. Analysis of the control G-V relationship gives us a minimum estimate of the total amount of charge that moves in the two-step transition from C_2 to O, but to use Eq. 5 we need to estimate z_1 and z_2, the charges that move in the C_2-C_1 and C_1-O transitions, respectively. The slope of the τ_{dea}–voltage relationship at the most negative voltages gives a measure of z_2, the gating charge that moves in the C_1 to O transition (cf. Liman, Hess, Weaver, and Koren, 1991). By subtracting z_2 from the total gating charge, we get an estimate of z_1.

(*b*) Estimating $V_{1/2}$. We have assumed that the $V_{1/2}$ for both activating steps is the same. It can readily be shown that at this potential the probability of channel opening in the steady state is ⅓. Therefore, we have estimated the $V_{1/2}$ of Eq. 5 as the voltage at which the conductance is ⅓ of the maximum. With an estimate of z and $V_{1/2}$ for each transition, we determined the value of β for each transition from its corresponding α using Eq. 5.

Estimating α_1, α_2, and a scaling factor. Finally, to fit the gating kinetics with the model we needed to estimate the parameters α_1, α_2, and a scaling factor that converts the fraction of open channels to a current. These were obtained by using a nonlinear least-squares iterative procedure to find the values of these parameters that best fit the data. Examples of the fits produced by this procedure are shown in Figs. 8 and 9, and demonstrate that the model can accurately describe SD channel gating kinetics.

FITTING THE ASCORBATE DATA

Having shown that the model fits the control kinetics, we next used it to analyze the SD channel activation kinetics in the presence of ascorbate. Our experimental results showed that ascorbate did not affect the kinetics of deactivation (Table II) or inactivation (Fig. 10). Therefore, in terms of the four-state model the C_1 to O transition and the O to I transition are unaffected by ascorbate, and to fit the ascorbate kinetic data we only needed to estimate α_1 and β_1 for the ascorbate-modified channels. All of the other parameters were the same as in control. The fraction of channels that were modified by ascorbate was obtained from the *G-V* curve in each cell, so that the activation kinetics in ascorbate could be fit by the appropriate fraction of unmodified and modified channels. One of the fits to the activation kinetics in ascorbate at +90 mV is shown in Fig. 9. As with the control data, the model accurately fits the ascorbate data. The values we obtained for α_1 of the ascorbate-modified channels at −10 and +90 mV are shown in Table IV. These averages are for the four cells for which activation kinetics *and G-V* curves were obtained. Ascorbate significantly decreases α_1 at +90 mV but not at −10 mV.

This modeling illustrates that the effects of ascorbate on SD channel gating are

TABLE IV

α_1 Rate Constant in Control and Ascorbate (n = 4)

Test pulse amplitude	Control α_1 ± SD	Ascorbate α_1 ± SD
	ms^{-1}	ms^{-1}
−10 mV	0.25 ± 0.16	0.23 ± 0.06
+90 mV	1.7 ± 0.13	0.89 ± 0.24

consistent with a simple gating model of the channel. In this simple four-state model, ascorbate decreases the forward rate of a voltage-dependent transition between two closed states of the channel, which produces a slowing of activation and a shift in the steady-state opening probability to more positive voltages. Interconversion between normal and modified channels is not required to explain our results.

Significance of SD Channel Modulation by Ascorbate

The functional role of SD calcium channels in rat pancreatic β cells has not been determined, but nonetheless we can speculate about the possible significance of SD channel inhibition by ascorbate. The decrease in the inward SD current could be significant in two regards. (*a*) It could change the rate of electrical firing activity. The SD channels, due to their lower activation threshold, have been suggested to be important in the pace-making activity of different cell types (Matteson and Armstrong, 1986; Hiriart and Matteson, 1988). Decreasing the rate of firing should decrease the amount of insulin secretion since the duration of the plateau potential and the amount of time the cells spend at the plateau potential are directly correlated with insulin secretion (Meissner and Preissler, 1980). (*b*) Inhibiting one of the routes of calcium entry into the cells could theoretically decrease the intracellular calcium

concentration and thereby decrease insulin secretion. We can further speculate that an ascorbate-induced decrease in insulin secretion could contribute to diabetes. Diabetes is a complex disease with undoubtedly many different etiologies. Our results suggest that the interaction of ascorbic acid and metals could be one mechanism whereby the diabetic condition may be exacerbated or even initiated.

Original version received 16 November 1992 and accepted version received 22 March 1993.

REFERENCES

Akaike, N., P. G. Kostyuk, and Y. V. Osipchuk. 1989. Dihydropyridine-sensitive low-threshold calcium channels in isolated rat hypothalamic neurones. *Journal of Physiology.* 412:181–195.

Armstrong, C. M., and F. Bezanilla. 1974. Charge movement associated with the opening and closing of the activation gates of the Na channel. *Journal of General Physiology.* 63:533–552.

Ashcroft, F. M., R. P. Kelly, and P. A. Smith. 1990. Two types of Ca channels in rat pancreatic B cells. *Pflügers Archiv.* 415:504–506.

Ashcroft, F. M., and P. Rorsman. 1989. Electrophysiology of the pancreatic β-cell. *Progress in Biophysics and Molecular Biology.* 54:87–143.

Bean, B. P. 1989. Neurotransmitter inhibition of neuronal calcium currents by changes in channel voltage dependence. *Nature.* 340:153–156.

Beech, D. J., L. Bernheim, and B. Hille. 1992. Pertussis-toxin and voltage dependence distinguish multiple pathways modulating calcium channels of rat sympathetic neurons. *Neuron.* 8:97–106.

Chatterjee, I. B., and A. Banerjee. 1979. Estimation of dehydroascorbic acid in blood of diabetic patients. *Analytical Biochemistry.* 98:368–374.

Chow, R. H. 1991. Cadmium block of squid calcium currents. Macroscopic data and a kinetic model. *Journal of General Physiology.* 98:751–770.

Elmslie, K. S., W. Zhou, and S. W. Jones. 1990. LHRH and GTP-γ-S modify calcium current activation in bullfrog sympathetic neurons. *Neuron.* 5:75–80.

Hille, B. 1992. Ionic Channels of Excitable Membranes. 2nd ed. Sinauer Associates, Inc., Sunderland, Ma. 55.

Hiriart, M., and D. R. Matteson. 1988. Na and two types of Ca channels in rat pancreatic beta cells identified with the reverse hemolytic plaque assay. *Journal of General Physiology.* 91:617–639.

Hirning, L. D., A. P. Fox, E. W. McCleskey, B. M. Olivera, S. A. Thayer, R. J. Miller, and R. W. Tsien. 1988. Dominant role of N-type Ca^{2+} channels in evoked release of norepinephrine from sympathetic neurons. *Science.* 239:57–61.

Hodgkin, A. L., and A. F. Huxley. 1952. A quantitative description of membrane current and its application to conduction and excitation in nerve. *Journal of Physiology.* 117:500–544.

Ikeda, S. R. 1991. Double-pulse calcium channel current facilitation in adult rat sympathetic neurones. *Journal of Physiology.* 439:181–214.

Kelly, R. P., R. Sutton, and F. M. Ashcroft. 1991. Voltage-activated calcium and potassium currents in human pancreatic β-cells. *Journal of Physiology.* 443:175–192.

Lacy, P. E., and M. Kostianovsky. 1967. Method for the isolation of intact islets of langerhans from the rat pancreas. *Diabetes.* 16:35–39.

Liman, E. R., P. Hess, F. Weaver, and G. Koren. 1991. Voltage-sensing residues in the S4 region of mammalian K^+ channel. *Nature.* 353:752–756.

Marchetti, C., E. Carbone, and H. D. Lux. 1986. Effects of dopamine and noradrenaline on Ca^{2+} channels of cultured sensory and sympathetic neurons of chick. *Pflügers Archiv.* 406:104–111.

Martell, A. E., and R. M. Smith. 1977. Critical Stability Constants. Vol. I. Amino Acids. Plenum Publishing Corp., New York. 495 pp.

Matteson, D. R., and C. M. Armstrong. 1986. Properties of two types of calcium channels in clonal pituitary cells. *Journal of General Physiology.* 87:161–182.

Meissner, H. P., and M. Preissler. 1980. Ionic mechanisms of the glucose-induced membrane potential changes in β-cells. *Hormone and Metabolic Research Supplement.* 10:91–99.

Nowycky, M. C., A. P. Fox, and R. W. Tsien. 1985. Three types of neuronal calcium channel with different calcium agonist sensitivity. *Nature.* 316:440–443.

Plant, T. D. 1988. Properties of calcium-dependent inactivation of calcium channels in cultured mouse pancreatic β-cells. *Journal of Physiology.* 404:731–747.

Ribalet, B., and P. M. Beigelman. 1980. Calcium action potentials and potassium permeability activation in pancreatic B-cells. *American Journal of Physiology.* 242:C296–C303.

Rorsman, P., and B. Hellman. 1988. Voltage-activated currents in guinea-pig pancreatic α_2-cells. *Journal of General Physiology.* 91:223–242.

Rorsman, O., and G. Trube. 1986. Calcium and delayed potassium currents in mouse pancreatic β-cells under voltage-clamp conditions. *Journal of Physiology.* 374:531–550.

Sala, S., and D. R. Matteson. 1990. Single-channel recordings of two types of calcium channels in rat pancreatic B-cells. *Biophysical Journal.* 58:567–571.

Samuni, A., J. Aronovitch, D. Godinger, M. Chevion, and G. Czapski. 1983. On the cytotoxicity of vitamin C and metal ions. *European Journal of Biochemistry.* 137:119–124.

Satin, L. S., and D. L. Cook. 1985. Voltage-gated inward currents in pancreatic islet β-cells. *Pflügers Archiv.* 404:385–387.

Som, S., S. Basu, S. Mukherjee, P. Deb, P. R. Choudhury, S. Mukherjee, S. N. Chatterjee, and I. B. Chatterjee. 1981. Ascorbic acid metabolism in diabetes mellitus. *Metabolism Clinical and Experimental.* 30:572–577.

Spires, S., and T. Begenisich. 1990. Modification of potassium channel kinetics by histidine-specific reagents. *Journal of General Physiology.* 96:757–775.

Stadtman, E. R. 1991. Ascorbic acid and oxidative inactivation of proteins. *American Journal of Clinical Nutrition.* 54:1125s–1128s.

Tsien, R. W., D. Lipscombe, D. V. Madison, K. R. Bley, and A. P. Fox. 1988. Multiple types of neuronal calcium channels and their selective modulation. *Trends in Neurosciences.* 11:431–438.

Winegar, B. D., R. Kelly, and J. B. Lansman. 1991. Block of current through single calcium channels by Fe, Co, and Ni. Location of the transition metal binding site in the pore. *Journal of General Physiology.* 97:351–367.